Sequence-Specific DNA Binding by the Glucocorticoid Receptor DNA-Binding Domain Is Linked to a Salt-Dependent Histidine Protonation†

Thomas Lundbäck,‡,§ Susanne van den Berg,‡ and Torleif Härd*,‖

Center for Structural Biochemistry, Department of Biosciences at Novum, Karolinska Institutet, and Department of Biotechnology, Royal Institute of Technology, Novum, S-141 57 Huddinge, Sweden

Received February 2, 2000; Revised Manuscript Received April 17, 2000

ABSTRACT: We used isothermal titration calorimetry in the temperature range 21−25 °C to investigate the effect of pH on the calorimetric enthalpy (ΔH_{cal}) for sequence specific DNA-binding of the glucocorticoid receptor DNA-binding domain (GR DBD). Titrations were carried out in solutions containing 100 mM NaCl, 1 mM dithiothreitol, 5% glycerol by volume, and 20 mM Tris, Hepes, Mops, or sodium phosphate buffers at pH 7.5. A strong dependence of ΔH_{cal} on the buffer ionization enthalpy is observed, demonstrating that the DNA binding of the GR DBD is linked to proton uptake at these conditions. The apparent increase in the pK_a for an amino acid side chain upon DNA binding is supported by the results of complementary titrations, where ΔH_{cal} shows a characteristic dependence on the solution pH. ΔH_{cal} is also a function of the NaCl concentration, with opposite dependencies in Tris and Hepes buffers, respectively, such that a similar ΔH_{cal} value is approached at 300 mM NaCl. This behavior shows that the DNA-binding induced protonation is inhibited by increased concentrations of NaCl. A comparison with structural data suggests that the protonation involves a histidine (His451) in the GR DBD, because in the complex this residue is located close to a DNA phosphate at an orientation that is consistent with a charged−charged hydrogen bond in the protonated state. NMR spectra show that His451 is not protonated in the unbound protein at pH 7.5. The pH dependence in ΔH_{cal} can be quantitatively described by a shift of the pK_a of His451 from approximately 6 in the unbound state to close to 8 when bound to DNA at low salt concentration conditions. A simple model involving a binding competition between a proton and a Na^+ counterion to the GR DBD−DNA complex reproduces the qualitative features of the salt dependence.

Studies of how solution conditions affect biomolecular interactions frequently lead to insights into the physical basis of the recognition process, especially if such data can be combined with structural information. Electrostatic interactions play an important role in DNA−protein binding equilibria, which consequently are sensitive to salt and pH conditions (see refs *1*−*3* and work cited therein). The approach to understand the role of electrostatics in DNA binding has therefore been to study the salt and pH dependence both experimentally and theoretically. For instance, recent results on the nonspecific DNA binding of the single-stranded DNA-binding (SSB) protein from *Escherichia coli* demonstrate complex linkages between pH and salt effects on protein−DNA interactions (*4*−*6*). It is clear from these studies that the distinction of various contributions to the experimentally observed free energy of binding ($\Delta G°_{obs}$) is improved if $\Delta G°_{obs}$ can be complemented by measurements of the binding enthalpy (ΔH).

Isothermal titration calorimetry (ITC)[1] provides a powerful tool for this type of studies (*7*, *8*), because the total calorimetric enthalpy (ΔH_{cal}) measured for a binding event contains contributions that depend not only on the interactions between the molecules but also on the composition of the buffer solution (*9*−*12*). In short, ΔH_{cal} for an interaction that involves a protonation/deprotonation of the interacting biomolecules will contain a contribution from the accompanying release or uptake of protons by the buffering substance. These events can therefore be probed by using the buffer reaction as a reporter and measuring ΔH_{cal} as a function of the buffering substance and/or the pH of the solution.

The objective of the present study is to examine the pH dependence, and how it is affected by the salt concentration, for sequence-specific DNA binding by the glucocorticoid receptor DNA-binding domain (GR DBD) by use of ITC. The data provide strong evidence for a shift in the pK_a of a histidine residue in the GR DBD upon DNA binding. As a

† This work was supported by the Swedish Natural Sciences Research Council (NFR) and the Magn. Bergvall Foundation.

* To whom correspondence should be addressed: e-mail Torleif.Hard@biochem.kth.se; phone +46-8-608 9230; fax +46-8-608 9290.

‡ Karolinska Institutet.

§ Present address: Pharmacia & Upjohn AB, Physical Chemistry, Structural Chemistry N62:5, S-112 87 Stockholm, Sweden. e-mail: Thomas.Lundback@eu.pnu.com.

‖ Royal Institute of Technology.

[1] Abbreviations: GR, glucocorticoid receptor; DBD, DNA-binding domain; GRE, glucocorticoid response element; DTT, dithiothreitol; ITC, isothermal titration calorimetry; ΔH_{cal}, calorimetric enthalpy; ΔH_d, heat of dilution and injection; ΔH_{ion}, ionization enthalpy; ΔH_0, binding enthalpy in the absence of protonation effects; Q_{obs}, observed fluorescence quenching; Q_{max}, maximum fluorescence quenching; pK_a, negative logarithm of ionization equilibrium constant; bp, base pair; K_{obs}, observed binding constant for protein monomer; *n*, binding stoichiometry; Tris, tris(hydroxymethyl)aminomethane; Hepes, *N*-(2-hydroxyethyl)piperazine-*N*′-2-ethanesulfonic acid; Mops, 3-(*N*-morpholino)-propanesulfonic acid.

10.1021/bi000231i CCC: $19.00
Published on Web 07/01/2000

result, DNA binding is coupled to proton uptake at neutral pH and low salt concentration conditions. This result is in very good agreement with the structure of the sequence-specific GR DBD−DNA complex (*13*) in which a histidine side chain is oriented so that it can form a charged−charged hydrogen bond with a DNA phosphate group.

MATERIALS & METHODS

Protein and DNA Preparation. The wild-type GR DBD (corresponding to the fragment K438−Q520 of the rat GR) was overproduced in *Escherichia coli* and purified as described previously (*14*) except for the gel-filtration step, which was performed in the buffers used for binding experiments as described below. The purified protein was extensively dialyzed at 4 °C against buffer A [100 mM NaCl, 1 mM dithiothreitol (DTT), and 5% glycerol by volume at pH 7.5], buffer B (10 mM Tris, 100 mM NaCl, 2 mM $MgCl_2$, 1 mM DTT, and 5% glycerol at pH 7.5), buffer C (10 mM Hepes, 100 mM NaCl, 2 mM $MgCl_2$, 1 mM DTT, and 5% glycerol at pH 7.5), or buffer D (150 mM NaCl, 2 mM $MgCl_2$, 1 mM DTT, and 5% glycerol at pH 7.5). The pH was measured on room temperature solutions (20−25 °C). Protein concentrations were determined spectrophotometrically with the extinction coefficient $\epsilon_{280nm} = 4200\ M^{-1}\ cm^{-1}$ calculated for tyrosine absorption (*15*).

The DNA-binding site (pGRE) consisting of two hexameric half-sites (highlighted in boldface type below) arranged as inverted repeats was incorporated into a 25-base pair oligomer (GCGTC **AGAACA** TGA **TGTTCT** AGGCG). This oligomer was synthesized and purified by high-pressure liquid chromatography (Cybergene, Huddinge, Sweden). An identical DNA fragment was used in a previous calorimetric study of GR DBD-DNA interactions (*19*). Following annealing of complementary strands, the DNA was dialyzed against buffer A, B, C, or D in the same beaker as the protein to avoid heat signals from mixing of nonequivalent buffers in the ITC experiments. The DNA concentration was determined spectrophotometrically by use of an average extinction coefficient $\epsilon_{260nm} = 13\ 200$ M (base pair^{-1}) cm^{-1} (*16*).

Isothermal Titration Calorimetry. Calorimetric titrations were carried out using the MCS ITC instrument from MicroCal Inc., Northampton, MA (see ref *7* for a description of the predecessor to this instrument). All solutions were carefully degassed before the titrations by use of the equipment provided with the calorimeter. GR DBD solutions (typically 0.1−0.3 mM) were titrated into pGRE solutions (typically 4−8 μM in DNA duplex) using the "250 μL" syringe, where each titration consisted of a preliminary 2 μL injection (neglected in the analysis) followed by 18 subsequent 15 μL additions. Heats of dilution and injection (ΔH_d) were measured in control experiments in which the protein solution was injected into buffer solution, and the magnitudes of these heats were similar to those observed at the end of the protein−DNA titrations. Measured heats of binding (ΔH_{cal}) were therefore corrected for the heats of dilution and injection by subtracting the average of the measured ΔH_d values. Differences in the observed magnitude of ΔH_d compared to ΔH_{cal} values observed at the end of the protein−DNA titrations were sometimes encountered and ΔH_{cal} was therefore additionally corrected in these cases by subtracting a value which in no case was larger than 0.8 kcal mol^{-1}. These small variations were ascribed to a combination of slightly different temperatures in the titration and the control experiments and imprecision in matching the buffer solution in the calorimeter cell and the injection syringe. At low salt concentration conditions, small differences compared to ΔH_d could also be a result of additional non-sequence specific DNA binding following saturation of the two specific half-sites.

Experiments were performed at different concentrations of NaCl by adding small amounts of stock solutions, prepared in buffer B or C, to protein and DNA samples in buffer B or C prior to the experiments. Experiments were performed at different pH conditions by adding small amounts (∼1%) of buffer stock solutions (0.8 M sodium phosphate, Tris, Mops, or Hepes) to protein and DNA samples in buffers A or D prior to the experiments. Protein and DNA concentrations used in the analysis of binding data were corrected for these small dilutions.

Fluorescence Spectroscopy. Fluorescence quenching experiments were performed as reverse titrations, in which DNA is titrated into a cell containing the protein solution. The extent of association is measured by following the DNA binding induced quenching of the intrinsic protein fluorescence. All experiments were carried out as described previously (*14*) with the following modifications. Protein and DNA stock solutions were dialyzed in buffer A and titrations were carried out at 25 °C with 10 mM Tris, pH 6.0−9.0, added to the solution. Each titration consisted of 24 successive 1.0 μL additions of the DNA stock solution into the cell containing protein at a concentration of 1.9 μM.

The concentration of bound protein was calculated from the fractional fluorescence quenching (Q_{obs}), defined as $(I_0 - I)/I_0$, where I_0 is the fluorescence intensity in the absence of DNA and I is the intensity in the presence of DNA. The concentration of bound GR DBD was determined as $C_B = (Q_{obs}/Q_{max})C_{tot}$, where C_B and C_{tot} are the bound and total GR DBD concentrations, respectively, and Q_{max} is the quenching observed when all protein is bound to DNA (see ref *17* for details).

Analysis of Binding Isotherms. The sequence-specific binding of GR DBD to a response element consisting of two hexameric half-sites arranged as inverted repeats can be described by a two-site cooperative model (*17*, *18*). Fluorescence data obtained with low (micromolar) reactant concentrations was fitted to obtain K_{obs} and Q_{max}, assuming a two-site model with a binding cooperativity of $\omega = 10$, as described previously (*19*). To analyze ITC experiments at higher reactant concentrations, one must consider that nonspecific binding can occur under low salt concentration conditions. In previously reported ITC experiments we have taken precautions to avoid this by increasing the salt concentration (*19*) to levels at which nonspecific binding is minimized (*17*). However, this was not possible in the present study since the objective was to investigate the linkage between pH and salt conditions, which requires studies also at low salt concentrations. In addition, it is difficult to resolve binding cooperativity in calorimetric experiments (*19*). We therefore evaluate ITC data using a simple model for noninteracting sites (see, e.g., ref *20*) in order to obtain an overall ΔH_{cal}, which represents an "effective" binding enthalpy for each of the monomers in the complex. The nonlinear least-squares fits of ITC data involved obtaining

best-fit values of the half-site binding constant (K_{obs}), stoichiometry (n), and ΔH_{cal}. In the analysis we focus on the binding enthalpy (ΔH_{cal}) determined in ITC experiments and binding affinities (K_{obs}) determined from fluorescence titrations. The calorimetrically determined enthalpy is only weakly, or not at all, affected by any nonsequence specific binding (see Results), whereas fluorescence titrations provide a more sensitive measure of changes in sequence-specific binding affinity because (i) they are carried out at lower reactant concentrations, where effects of weaker nonspecific binding are reduced, (ii) the (micromolar) binding affinity is more accurately determined at these concentration conditions, and (iii) the change in signal is similar at all pH values in the fluorescence experiments, ensuring that the comparison of binding isotherms is not affected by the sensitivity (signal-to-noise ratio). The thermodynamic quantities determined in this study are based on the total macromolecular concentrations, neglecting nonideality of the solution, and they are therefore valid only at the specified conditions.

NMR Spectroscopy. NMR spectroscopy was performed on a Varian Unity 500 spectrometer at a magnetic field of 11.74 T. The GR DBD sample used for NMR (~3 mM) was dialyzed against a buffer containing 100 mM NaCl, 2 mM $MgCl_2$, and 1 mM DTT at pH 7.0. The sample was quickly frozen in liquid nitrogen and lyophilized to remove the water, followed by a resuspension in 20 mM deuterated Tris and 2 mM DTT in D_2O at pH* = 6.0, where pH* refers to the reading of the pH meter. The pH* was carefully raised by addition of small aliquots of NaOD in D_2O and an NMR spectrum was recorded at each pH*. At the titration end point (pH* $\approx$ 8.2), the concentration of NaCl was increased to 300 mM by addition of NaCl (4.5 M in D_2O) and the pH* was subsequently lowered to enable a similar pH titration at the higher salt concentration.

RESULTS

We applied ITC to characterize the pH dependence of ΔH_{cal} for sequence-specific DNA binding of GR DBD. Protonation effects can be investigated by comparing ΔH_{cal} for the binding event in buffers with different enthalpies of ionization (ΔH_{ion}). If the association involves a change in the protonation state of the reactants, then ΔH_{cal} is expected to contain a term proportional to the ionization enthalpy of the buffer (*9*−*12*):

$$\Delta H_{cal} = \Delta H_{bind} + \Delta n_{H^+} \Delta H_{ion} \quad (1)$$

where Δn_{H^+} is the number of protons released by the buffer and ΔH_{bind} is the binding enthalpy resulting from interactions between the macromolecules, i.e., the enthalpy that would be observed in a solution where ΔH_{ion} is zero.

Raw data from calorimetric titrations of pGRE with GR DBD in buffer A with either Tris, Mops, or sodium phosphate are shown in Figure 1A. The calorimetric response clearly depends on the nature of the buffering substance because the association reaction is endothermic with Tris and exothermic with sodium phosphate, whereas the Mops buffer results in a very small difference compared to the blank titration. Figure 1B shows the corresponding integrated data corrected for heats of dilution and injection.

The experiments in Figure 1 were carried out at a relatively low salt concentration (100 mM) where additional non-sequence specific DNA binding can occur (*17*). It is therefore important to establish whether this has any significant impact on ΔH_{cal}. We argue that if non-sequence specific binding occurs at these conditions it must be associated with an undetectable binding enthalpy, for two reasons. First, the observed binding stoichiometry is close to 2 in all ITC experiments (average $n = 1.87 \pm 0.23$ for all experiments), indicating that essentially only binding to the two specific half-sites is detected. Second, the heats observed for injections at the end of the protein−DNA titrations are similar to those observed throughout the control experiments (Figure 1A) and in the different buffers. Hence, if non-sequence specific DNA binding occurs, it must be associated with an undetectably small enthalpy change, which does not change significantly with the buffering substance. These observations imply that the ITC data can be used at all conditions to obtain an accurate ΔH_{cal} for sequence-specific DNA binding of the GR DBD.

The ITC binding isotherms show no significant difference in signal (enthalpy) for the binding of the first and second GR DBD molecules to the dimeric site on pGRE (Figure 1; see also ref *19*). The theoretical possibility that the GR DBD binds DNA as a preformed dimer can be excluded because NMR data clearly show that the protein is monomeric at concentrations that are almost 2 orders of magnitude higher than that in the calorimetry reaction cell (*21*−*23*). Furthermore, we only detect binding of a GR DBD monomer in gel mobility shift assays with DNA oligomers with a single half-site, whereas both monomers and dimers are observed bound to oligomers containing the correct inverted repeat of half-sites, e.g., the pGRE sequence (*14*). Any binding cooperativity is therefore either associated with a small enthalpy change or too weak to be detected under the present conditions. These observations support a quantitative evaluation of ITC data by use of a simple model with noninteracting binding sites, and this procedure yields a robust estimate of the overall ΔH_{cal} for binding of each GR DBD monomer to pGRE, as demonstrated in Figure 1B.

The dependence of ΔH_{cal} on the buffering substance is further illustrated in Figure 2, where ΔH_{cal} is plotted as a function of the buffer ionization enthalpy, ΔH_{ion}, in buffers containing either 100 mM NaCl (buffer A) or 100 mM NaCl and 2 mM $MgCl_2$ (buffers B and C). The plots reveal an approximately linear dependence with buffer A as expected from eq 1. We estimate that the binding of each GR DBD molecule at these conditions (100 mM NaCl and pH 7.5) is associated with an uptake (Δn_{H^+}) of approximately 1 proton. Fewer data points were obtained in $MgCl_2$-containing buffers. Still, the lower ΔH_{cal} value obtained with Tris suggests that a somewhat smaller fraction of protons ($\Delta n_{H^+} \approx 0.7$) is absorbed per bound protein in the presence of $MgCl_2$. The analysis of protonation effects assumes that the different buffers do not interact with the macromolecules, and the linear appearance of a plot of ΔH_{cal} vs ΔH_{ion} in buffer A supports this assumption (Figure 2).

The salt concentration dependence of ΔH_{cal} was investigated by ITC titrations in Tris and Hepes buffers (with 2 mM $MgCl_2$) at NaCl concentrations ranging from 100 to 300 mM. The results (Figure 3) show that the ΔH_{cal} depends strongly on the NaCl concentration in both buffers. The dependence is consistent with a change in protonation from approximately 0.7 per GR DBD molecule at 100 mM NaCl

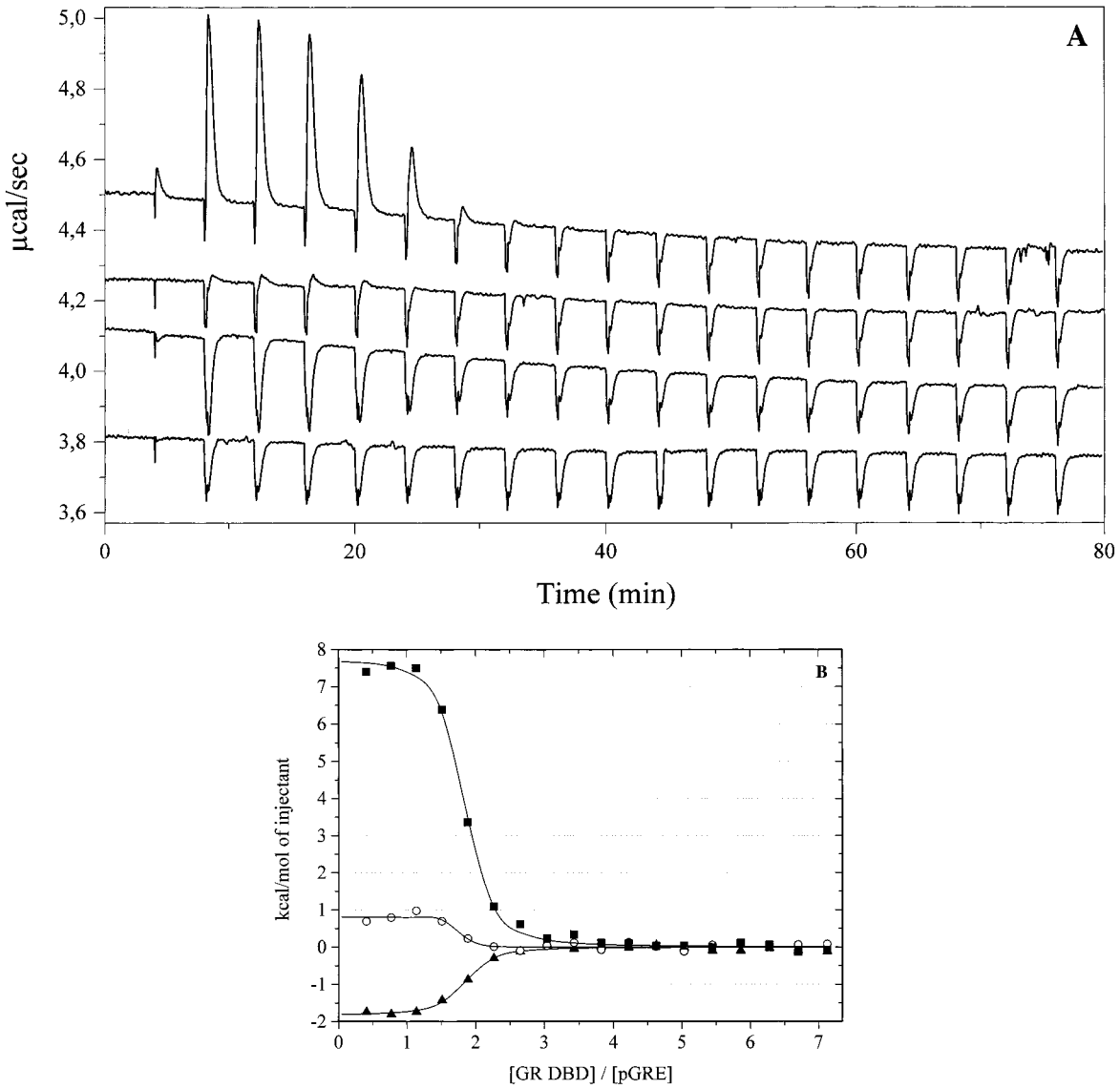

FIGURE 1: (A) Calorimetric titrations of pGRE (5.6 μM) with GR DBD (0.23 mM) at 20.9−22.5 °C in buffer A with 20 mM Tris (top), Mops (upper middle), or sodium phosphate (lower middle) at pH 7.5, and a control experiment in which the GR DBD solution is injected into buffer A with 20 mM Tris at pH 7.5 (bottom). (B) Corresponding integrated heats of binding corrected for heat of dilution and injection for Tris (■), Mops (○), and sodium phosphate (▲), respectively. Solid lines represent the best-fit binding isotherms as described in the Materials and Methods section.

to close to zero at 300 mM NaCl. The inset in Figure 3 shows a plot of ΔH_{cal} vs buffer ΔH_{ion} at three salt concentrations. The lines that are drawn between data points have a fairly well defined point of intersection at a position where ΔH_{ion} equals 6−7.3 kcal/mol. In the absence of fortuitous compensation, this value corresponds to the reaction enthalpy for the DNA binding-induced protonation (*12*). The narrow dispersion of intersection points also implies that the protonation reaction enthalpy is relatively independent of salt concentration in the range 100−300 mM NaCl.

An alternative approach to investigate protonation effects in association reactions is to examine the effect of pH on ΔH_{cal}. We therefore carried out titrations of pGRE with GR DBD in buffer D to which we added 10 mM Tris-HCl with pH values ranging from 6.5 to 9.0. It was not possible to obtain data at pH > 9 due to precipitation, and the titrations were not carried out at lower pH values because the GR DBD is known to lose two structurally important zinc ions at low pH (*24*). Still, the results (Figure 4) demonstrate a clear pH dependence: ΔH_{cal} appears to go through a maximum close to pH 7.0, indicating that the extent of DNA binding-induced protonation is optimal at this pH. The buffering capacity of the Tris solution becomes lower at pH values far from the pK_a (=8.03 at 25 °C; *25*). A net release from the buffer of a majority of the protons taken up by the protein upon DNA binding is still expected also at pH 6.5 because of the large excess of Tris compared to alternative buffering substances. The solution pH is also expected to change when Tris becomes deprotonated at a pH value where its buffering capacity is less than optimal. However, calculations of this effect show that it is negligible (less than 0.02 pH units). The absence of clear end points on the pH curve complicates the determination of pK_a for the protonated group in the bound and unbound state, but when complemented with other observations, these data can be rationalized as described in the Discussion.

Measured reaction enthalpies indicate a shift in the pK_a of an ionizable group in the GR DBD upon DNA binding.

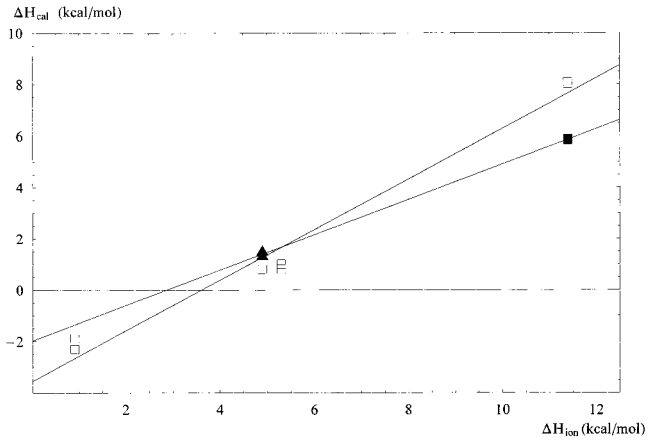

FIGURE 2: Calorimetric enthalpy ΔH_{cal} for the binding of GR DBD to pGRE as a function of ΔH_{ion} for the buffering substance. (Each data point in Figures 2−4 represents a separate titration.) Included in the plot are data from experiments in buffer A with 20 mM Tris, Hepes, Mops, or sodium phosphate at pH 7.5 (□) and in the $MgCl_2$-containing buffers B (■) and C (▲). ΔH_{ion} was taken as 11.39 kcal mol^{-1} for Tris (*25*), 5.01 kcal mol^{-1} for Hepes (*27*), 5.3 kcal mol^{-1} for Mops (*28*), and 0.9 kcal mol^{-1} for sodium phosphate (*25*). These values refer to the tabulated data at 25 °C and in the presence of salt when this has been specified. The solid lines represent linear regression analyses of the data and have slopes of 0.98 (correlation coefficient $r^2 = 0.973$) and 0.69 for data in the absence and presence of $MgCl_2$, respectively.

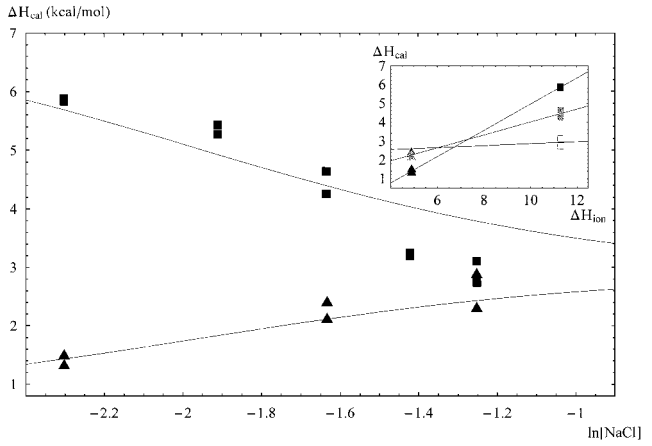

FIGURE 3: ΔH_{cal} for the binding of GR DBD to pGRE at 21.0−23.1 °C in buffers B (■) and C (▲) at different NaCl concentrations. The ITC experiments in buffer B were carried out with 0.10 mM GR DBD in the injection syringe and 5.8 μM pGRE in the cell, whereas 0.17 mM GR DBD and 8.1 μM pGRE were used for the experiments in buffer C. The solid lines describe a model in which the proton competes with a Na^+ cation for binding at the macromolecular interface (see Discussion). The inset shows ΔH_{cal} as a function of ΔH_{ion} for the buffering substance (see legend to Figure 2 for ΔH_{ion} values). The solid lines represent linear regression analyses of the data and have slopes of 0.70 at 100 mM NaCl (solid symbols), 0.34 at 200 mM NaCl (gray symbols), and 0.05 at 300 mM NaCl (open symbols), respectively.

This shift can be expected to be reflected also in a pH dependence of the binding affinity. To investigate this, we performed complementary fluorescence titrations in which the DNA binding of the GR DBD was followed in buffer A with 10 mM Tris, with pH in the range 6.0−9.5 (Figure 5). These titrations show that the overall binding depends strongly on pH with significantly higher affinities at lower pH, as expected on the basis of the ITC data. Best-fit binding constants (Figure 5, inset) decrease with more than 1 order

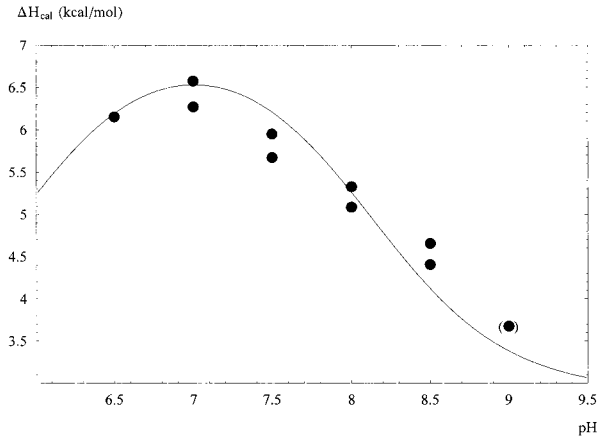

FIGURE 4: ΔH_{cal} for the binding of GR DBD to pGRE as a function of pH in buffer D with 10 mM Tris. The ITC experiments were carried out at 21.7−24.7 °C with 0.26 mM GR DBD in the injection syringe and 5.7 μM pGRE in the cell. The data point at pH 9.0 is treated as uncertain, because a precipitation was observed when the sample was taken out of the ITC cell. The solid line represents the best fit of a model in which a histidine residue becomes protonated upon DNA binding as described in the Discussion. (The data point at pH 9.0 was not used in this fit.)

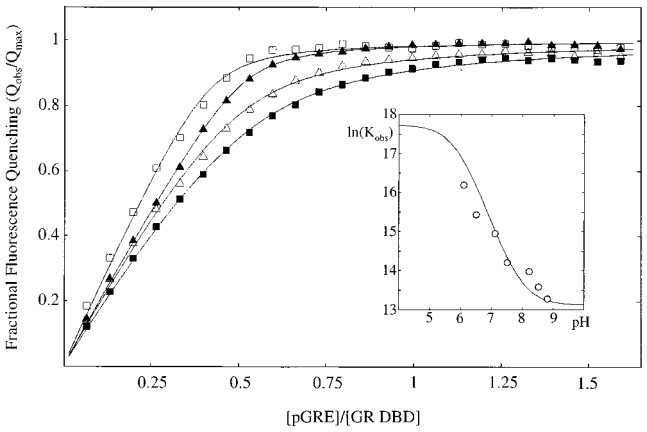

FIGURE 5: Fractional fluorescence quenching as a function of total molar ratio for reverse titrations of GR DBD with pGRE at 25 °C in buffer A with 10 mM Tris at pH 6.0 (□), 7.0 (▲), 8.0 (△), or 9.0 (■). The solid lines represent the best fit of theoretical binding isotherms to experimental data as described in the Materials and Methods section. The inset shows the natural logarithm of best-fit values of the binding constant K_{obs} for a two-site model with a cooperativity parameter $\omega = 10$ (*14*). The solid line describes the expected pH dependence of the binding constant if the pK_a of an ionizable group in the GR DBD is shifted from 5.9 to 7.9 upon binding (see Discussion).

of magnitude in the pH interval 6.1−8.8. The fit to a two-site model is not perfect at low pH, especially at the beginning of the titrations, where there is a large excess of protein in the solution. This could indicate that nonspecific binding occurs. However, the deviation can equally well be attributed to uncertainties in measured protein concentrations, which become critical when the binding reaction is nearly quantitative. A calculation of the effect of nonspecific binding with known binding parameters and their salt dependence (*17*) shows that a "worst-case scenario" with nonspecific binding affinity on the order of 1×10^5 M^{-1} (at pH = 7.5) would yield errors in the fluorescence quenching that are lower than those from other uncertainties such as concentration and measurement imprecision. Hence, any influence of nonspecific binding on the interpretation is small, and the

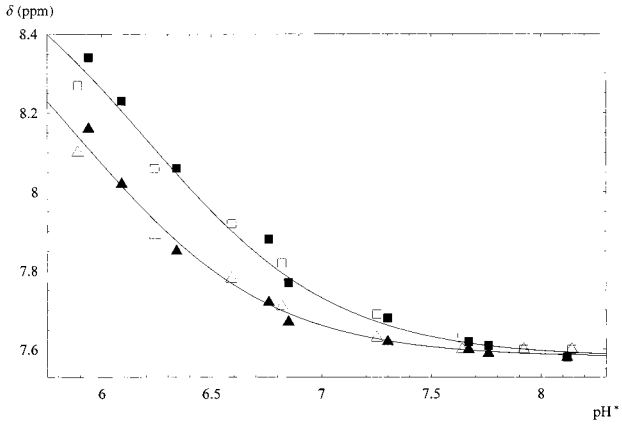

FIGURE 6: Chemical shifts (δ) of the $H^{\epsilon 1}$ protons in His451 (triangles) and His472 (squares) in GR DBD as a function of pH*. The experiments were carried out in D_2O with 20 mM deuterated Tris, 2 mM $MgCl_2$, 1 mM DTT, and 100 mM NaCl (solid symbols) or 300 mM NaCl (open symbols). The solid lines indicate the predicted behavior for protonations with pK_a equal to 5.9 and 6.2 for His 451 and His 472, respectively, with the chemical shift changing from 8.69 to 7.58 when these residues become deprotonated.

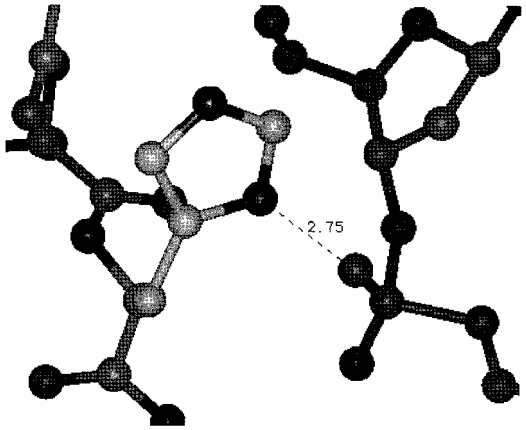

FIGURE 7: Part of the protein−DNA interface in the complex between GR DBD and a GRE (*13*). The drawing illustrates the protein backbone (left) with the $H^{\delta 1}$ proton on the His451 side chain at hydrogen-bonding distance (2.75 Å) to a phosphate group on the DNA (right). A protonation of the histidine is required for the formation of an intermolecular charged−charged hydrogen bond.

fluorescence equilibrium titrations afford a qualitative confirmation of the expected pH dependence at low salt concentrations.

Considering the pH range within which ΔH_{cal} varies, we suspected that the protonation involves a histidine residue in the protein. We therefore used NMR spectroscopy to estimate the pK_a of the two histidine residues in the unbound state of the GR DBD. The NMR chemical shifts of the two resolved $H^{\epsilon 1}$ resonances depend on pH (Figure 6), and this reflects changes in histidine protonation states within the investigated pH interval (*26*). It is difficult to obtain a precise measure of the pK_a of these histidines in the absence of a clear low-pH end point. However, the proton resonances were also significantly broadened in the mixed protonation state (not shown), and from this effect it is possible to see that His472 is past the titration midpoint at pH 5.9, while His451 is still broad at pH 5.9 (the numbering of residues refers to the rat GR). From these data we estimate approximate pK_a values in the unbound protein of 5.9 and 6.2 for His451 and His472, respectively. It is also clear that the pK_a of the histidines in the unbound protein is relatively independent of salt concentration in the range 100−300 mM NaCl (Figure 6). Unfortunately, it was not possible to record the corresponding NMR spectra of the GR DBD−DNA complex due to solubility problems at the required concentration conditions.

DISCUSSION

We used ITC and fluorescence titrations to investigate how sequence-specific DNA binding by the GR DBD depends on pH and salt concentration conditions. Calorimetrically measured binding enthalpies observed with different buffers demonstrate that complex formation is accompanied by a coupled protonation reaction. The effects of pH and salt are linked such that the (pH-dependent) protonation is inhibited when the NaCl concentration is increased. These observations establish that the pK_a of an ionizable group is shifted to higher values when the complex is formed, with the magnitude of this shift being dependent on the salt concentration. Below we examine the molecular basis for the observed effect. We then quantify the pH-dependent binding enthalpy and provide a qualitative model of the linked salt and pH effects. Finally, we briefly discuss any impact on the interpretation of previously measured heat capacity changes upon GR DBD−GRE complex formation.

pH-Dependent Binding Enthalpy Is Due to a Shift in the pK_a of His451. The effect that we observe occurs in the pH interval 6−8, which suggests that the binding induced protonation involves a histidine residue in the GR DBD, because the (lower) pK_a for histidine in water is around 6.0 (*25*). A comparison with available structural data (*13*) supports this interpretation (Figure 7): His451 is located within hydrogen-bonding distance of a DNA phosphate group in a sequence-specific GR DBD−DNA complex, and a protonation of this histidine would be required for the formation of a charged−charged intermolecular hydrogen bond. Furthermore, an estimate of ΔH_{ion} in the range 6−7.3 for the protonated group in the complex can be obtained from the common point of intersection of the three lines in the inset to Figure 3. Within experimental uncertainty, this value is close to the literature value for histidine protonation enthalpy, which equals 7.14 kcal mol^{-1} (*25*).

The GR DBD also contains two cysteine residues that are not involved in zinc coordination. One of these is exposed close to the DNA binding surface and must also be considered as a potential candidate for protonation. On the other hand, cysteine in water has a pK_a of 8.39 and a ΔH_{ion} of 8.6 kcal mol^{-1} (*25*). These numbers are both significantly different from our experimental observations. We therefore favor the interpretation involving a protonation of the histidine residue at the protein−DNA interface, especially in light of the observed protein−DNA interaction in the crystal structure of the complex.

Quantification of the pH Effect. It is possible to quantitatively account for the pH dependence of ΔH_{cal} reported in Figure 3 by use of the literature value for histidine protonation. For this evaluation we also need an estimate of ΔH_{cal} for the protein−DNA association in the absence of protonation effects (referred to as ΔH_0). There are two ways to obtain this number from experimental data. A first estimate of $\Delta H_0 \approx 2.8$ kcal mol^{-1} can be obtained from Figure 3 at

high salt concentration conditions, where similar reaction enthalpies in Tris and Hepes buffers indicate that protonation effects do not occur. To use this value we must assume that ΔH_{cal} is independent of salt concentration in the absence of protonation. The assumption is consistent with an entropically dominated salt dependence of protein−DNA interactions (*1*). We note that salt effects are not purely entropic in some cases that involve direct interactions between the ions and the macromolecules (*4*−*6*). Still, our assumption is also supported by a common point of intersection of plots of ΔH_{cal} versus ΔH_{ion} at different salt concentrations (inset in Figure 3). This is because such a behavior would not be observed unless ΔH_{ion} for the DNA binding-induced protonation does not change by more than ca. 1 kcal mol^{-1} with the NaCl concentration and unless ΔH_0 is relatively independent of salt concentration, i.e., changes by less than ca. 1 kcal mol^{-1} between 100 and 300 mM NaCl. A second estimate can be obtained from the fit of eq 1 to data in Figure 2, which yields $\Delta H_0 = 3.0$ kcal mol^{-1}. The two estimates of ΔH_0 agree well despite the fact that they are based on data obtained at different salt concentrations, which supports our assumptions, and we use the average value, $\Delta H_0 = 2.9$ kcal mol^{-1}, in our calculations. The pH dependence of ΔH_{cal} can be described by (adopted from ref *12*)

$$\Delta H_{cal} = \Delta H_0 + (\Delta H_{ion}^{Tris} - \Delta H_{ion}^{His})\left(\frac{10^{(pK_a^{bound}-pH)}}{1+10^{(pK_a^{bound}-pH)}} - \frac{10^{(pK_a^{free}-pH)}}{1+10^{(pK_a^{free}-pH)}}\right) \quad (2)$$

where ΔH_{ion}^{Tris} (11.39 kcal mol^{-1}; *25*) and ΔH_{ion}^{His} are the ionization enthalpies of Tris and histidine (assumed here to be the same in the unbound and bound states), pK_a^{bound} and pK_a^{free} (5.9; taken from the NMR experiments) are the negative logarithms of the apparent ionization constants for His451 in the bound and unbound state, and the two terms within the second parentheses represent fractional protonation in bound and free states, respectively. A fit of eq 2 qualitatively reproduces experimental data with $pK_a^{bound} = 8.1$, as illustrated by the solid line in Figure 4.

Equation 2 can be used to describe ΔH_{cal} at all NaCl concentrations and in different buffers (Figure 3), provided that the salt dependence of pK_a^{bound} is considered and the correct ΔH_{ion} is used for the buffering substance. This is because ΔH_{ion} for histidine falls between the corresponding values for Tris and Hepes, i.e., a coupled protonation will give an exothermic contribution to ΔH_{cal} in the Hepes buffer and endothermic contribution in the Tris buffer. A lowering of the salt concentration results in a DNA binding-induced proton uptake, which leads to a reduced magnitude of the endothermic enthalpy in Hepes but an opposite increase in Tris (Figure 3). Assuming that ΔH_0 remains constant with ionic strength, eq 2 can be used to obtain estimates of pK_a^{bound} at the various NaCl concentrations in the presence of both buffers. A consistency between these values will only be encountered if the correct ΔH_{ion} for the protonated group is used. With $\Delta H_0 = 2.9$ kcal mol^{-1}, $\Delta H_{ion}^{Tris} = 11.39$ kcal mol^{-1}, $\Delta H_{ion}^{Hepes} = 5.01$ kcal mol^{-1} (*27*), $\Delta H_{ion}^{His} = 7.14$ kcal mol^{-1}, and $pK_a^{free} = 5.9$, we calculate pK_a^{bound} values of 7.9 in Tris and 7.9 in Hepes buffers at 100 mM NaCl, 7.3 and 7.2 at 200 mM NaCl, and 6.0 and 6.8 at 300 mM NaCl. The pK_a^{bound} value obtained in this way for 100 mM NaCl (7.9) is in good agreement with that obtained by fitting the pH dependence of binding enthalpies in Tris buffer (8.1). There is also a very good agreement between values calculated for Tris and Hepes buffers, except at 300 mM NaCl. This latter discrepancy results at least partly from a larger sensitivity to the choice of reference ΔH_0, since the experimental uncertainty at 300 mM NaCl is larger than the difference between ΔH_0 and ΔH_{cal}. (The experimental uncertainty in ΔH_{cal} increases with reduced affinities; see, e.g., Figure 3). The agreement between pK_a^{bound} values obtained in the two buffers provides further evidence that the salt dependence of ΔH_{cal} can be explained by the protonation of a histidine residue, for which pK_a^{bound} depends on the salt concentration.

The calculated shift in pK_a is consistent with the observed pH dependence in binding affinity as monitored in the fluorescence titrations, as shown in the inset in Figure 5. The pH-dependent binding affinity, K, is given by

$$\ln(K) = \ln(K_0) + \ln(1+10^{(pK_a^{bound}-pH)}) - \ln(1+10^{(pK_a^{free}-pH)}) \quad (3)$$

where K_0 is the binding constant of the unprotonated protein. This relation qualitatively reproduces measured K_{obs} values in the pH range 6−9, given that $pK_a^{free} = 5.9$ and $pK_a^{bound} = 7.9$ and assuming a value of $K_0 = 5 \times 10^5$ M^{-1}.

Simple Model for Combined pH and Salt Concentration Effects. As a first approximation, the linkage between a protonation reaction and the salt concentration can be modeled as a competition between a proton and a cation for the available site at the protein−DNA interface (compare Figure 7). According to the ion release theory (*1*), the addition of an additional positive charge on the interacting macromolecule will facilitate the binding to DNA due to the entropic release of additional DNA-associated counterions. An increase of the salt concentration will consequently drive the complex toward the deprotonated state because (i) the release of a counterion, which is a direct consequence of proton binding in this model, becomes less favorable at higher salt concentrations and (ii) the counterion competes with the proton for the space at the interface where favorable interactions between ionic and polar groups are possible.

The competition between the proton and a Na^+ counterion can be illustrated by the following thermodynamic cycle:

$$\begin{array}{ccc} DNA\cdot Na^+ + H^+\cdot DBD & \xleftrightarrow{K_a^{free}} & DNA\cdot Na^+ + DBD + H^+ \\ \updownarrow K_{low\,pH}^{low\,salt} & & \updownarrow K_{high\,pH}^{high\,salt} \\ DNA\cdot H^+\cdot DBD + Na^+ & \xleftrightarrow{K'^{bound}_a} & DNA\cdot Na^+\cdot DBD + H^+ \end{array}$$

where $K_{lowpH}^{lowsalt}$ and $K_{highpH}^{highsalt}$ represent observed binding constants for the protein−DNA complexation at the indicated conditions and $K'_a{}^{bound}$ is the apparent ionization constant for the complex when counterion competition is considered. It should be pointed out that protein binding probably displaces several counterions. This reaction is assumed to remain unaffected by the histidine protonation, which is why only a single counterion on DNA is indicated in the cycle. A relation between $K'_a{}^{bound}$ and K_a^{free} can be obtained by considering the cycle and applying counterion condensation

theory (*1*) to find a relation between $K_{\text{lowpH}}^{\text{lowsalt}}$ and $K_{\text{highpH}}^{\text{highsalt}}$:

$$\frac{K'_{\text{a}}{}^{\text{bound}}}{K_{\text{a}}^{\text{free}}} = \frac{K_{\text{highpH}}^{\text{highsalt}}}{K_{\text{lowpH}}^{\text{lowsalt}}} = k[\text{Na}^+]^{0.88} \quad (4)$$

where

$$\text{p}K'_{\text{a}}{}^{\text{bound}} = \text{p}K_{\text{a}}^{\text{free}} - \log k - 0.88 \log [\text{Na}^+]$$

Here, $[\text{Na}^+]^{0.88}$ reflects the additional counterion released by GR DBD with a protonated histidine compared to the deprotonated protein and the parameter k represents the ratio of the binding constants for formation of complexes with a proton or a Na^+ cation at the interface, at a hypothetical standard state of 1 M salt.

The competition between a proton and a counterion, i.e. the bottom reaction in the cycle, results in a fractional protonation of the protein in the complex ($\bar{H}^{\text{bound}}$) according to

$$\bar{H}^{\text{bound}} = \frac{\text{DNA}\cdot\text{H}^+\cdot\text{DBD}}{\text{DNA}\cdot\text{H}^+\cdot\text{DBD} + \text{DNA}\cdot\text{Na}^+\cdot\text{DBD}} = \frac{K'_{\text{a}}{}^{\text{bound}} a_{\text{H}^+}}{K'_{\text{a}}{}^{\text{bound}} a_{\text{H}^+} + [\text{Na}^+]} \quad (5)$$

where a_{H^+} is the H^+ activity. Equations 4 and 5 can be combined and subsequently used to replace the term for $\bar{H}^{\text{bound}}$ (first term in the second parentheses) in eq 2. For $k = 1$, this results in an expected salt dependence as illustrated by the two solid lines in Figure 3. It is clear that the competition model with $k = 1$ cannot fully account for the strong salt effect on protonation. However, the model is simple and does not take into account further complications such as competition by 2 mM Mg^{2+} in the experimental buffer.

Heat Capacity Effects. The protonation effect will provide a small contribution to the apparent heat capacity change for the binding reaction (*12*). We previously demonstrated an agreement between the observed heat capacity change and the value expected on the basis of changes in accessible surface area in the GR DBD−GRE complex (*19*). However, the protonation was not considered in this study and this warrants a further examination of the expected effect. The temperature dependence experiments (*19*) were carried out in 50 mM Hepes at pH 7.4 with a total concentration of 225 mM monovalent cations. On the basis of the present results, we expect only a weak protonation effect at this salt concentration. However, to estimate the largest possible contribution we assume that $\text{p}K_{\text{a}}{}^{\text{bound}}$ equals the pH at these conditions. Adopting eqs 10−12 in ref *12*, we estimate a contribution to the heat capacity change of 0.027 kcal mol^{-1} K^{-1} for the protonation event using the following parameters: pH = 7.4; $\text{p}K_{\text{a,c}} = 7.4$; $\text{p}K_{\text{a,f}} = 5.9$; $\Delta H_{\text{p}}{}^{\text{f}} = -7.14$ kcal mol^{-1}; $\delta\Delta H_{\text{f}} = 0$ kcal mol^{-1}; $\Delta C_{p,\text{p}}{}^{\text{f}} = 3.8$ cal mol^{-1} K^{-1}; $\delta\Delta C_{p,\text{p}} = 0$ cal mol^{-1} K^{-1}; $\Delta H_{\text{i}}{}^{b} = 4.9$ kcal mol^{-1}; and $\Delta C_{p,\text{i}}{}^{b} = 11.7$ cal mol^{-1} K^{-1}, where the notation is the same as in our previous paper (*19*). This number is small compared to the observed heat capacity change, −0.26 kcal mol^{-1} K^{-1}, and does not affect the conclusion that heat capacity changes in the present association reaction agree with calculations based on changes in solvent-accessible surface area.

ACKNOWLEDGMENT

We thank Dr. Barry Honig, Columbia University, for valuable discussions.

REFERENCES

1. Record, M. T., Ha, J.-H., and Fisher, M. A. (1991) *Methods Enzymol. 208*, 291−343.
2. Misra, V. K., Hecht, J. L., Sharp, K. A., Friedman, R. A., and Honig, B. (1994) *J. Mol. Biol. 238*, 264−280.
3. Härd, T., and Lundbäck, T. (1996) *Biophys. Chem. 62*, 121−139.
4. Overman, L. B., and Lohman, T. M. (1994) *J. Mol. Biol. 236*, 165−178.
5. Lohman, T. M., Overman, L. B., Ferrari, M. E., and Kozlov, A. G. (1996) *Biochemistry 35*, 5272−5279.
6. Kozlov, A. G., and Lohman, T. M. (1998) *J. Mol. Biol. 278*, 999−1014.
7. Wiseman, T., Williston, S., Brandts, J. F., and Lin, L.-N. (1989) *Anal. Biochem. 179*, 131−137.
8. Freire, E., Mayorga, O. L., and Straume, M. (1990) *Anal. Biochem. 62*, 950−959.
9. Eftink, M., and Biltonen, R. (1980) in *Biological Microcalorimetry* (Beezer, A., Ed.) pp 343−412, Academic Press, San Diego, CA.
10. Takahashi, K., and Fukada, H. (1985) *Biochemistry 24*, 297−300.
11. Doyle, M. L., Louie, G., Monte, P. R. D., and Sokoloski, T. D. (1995) *Methods Enzymol. 259*, 183−194.
12. Baker, B. M., and Murphy, K. P. (1996) *Biophys. J. 71*, 2049−2055.
13. Luisi, B. F., Xu, W. X., Otwinowski, Z., Freedman, L. P., Yamamoto, K. R., and Sigler, P. B. (1991) *Nature 352*, 497−505.
14. Lundbäck, T., Zilliacus, J., Gustafsson, J.-Å., Carlstedt-Duke, J., and Härd, T. (1994) *Biochemistry 33*, 5955−5965.
15. Cantor, C. R., and Schimmel, P. R. (1980) *Biophysical Chemistry, Part II*, W. H. Freeman and Company, New York.
16. Mahler, H. R., Kline, B., and Mehrota, B. D. (1964) *J. Mol. Biol. 9*, 801−811.
17. Härd, T., Dahlman, K., Carlstedt-Duke, J., Gustafsson, J.-Å., and Rigler, R. (1990) *Biochemistry 29*, 5358−5364.
18. Dahlman-Wright, K., Siltala-Roos, H., Carlstedt-Duke, J., and Gustafsson, J.-Å. (1990) *J. Biol. Chem. 265*, 14030−14035.
19. Lundbäck, T., and Härd, T. (1996) *Proc. Natl. Acad. Sci. U.S.A. 93*, 4754−4759.
20. Wyman, J., and Gill, S. J. (1990) *Binding and Linkage: Functional Biochemistry of Biological Macromolecules*, Chapter 2, University Science Books, Mill Valley, CA.
21. Härd, T., Kellenbach, E., Boelens, R., Maler, B. A., Dahlman, K., Freedman, L. P., Carlstedt-Duke, J., Yamamoto, K. R., Gustafsson, J.-Å., and Kaptein, R. (1990) *Science 249*, 157−160.
22. Berglund, H., Kovács, H., Dahlman-Wright, K., Gustafsson, J.-Å., and Härd, T. (1992) *Biochemistry 31*, 12001−12011.
23. Baumann, H., Paulsen, K., Kovács, H., Berglund, H., Wright, A. P. H., Gustafsson, J.-Å., and Härd, T. (1993) *Biochemistry 32*, 13463−13471.
24. Zilliacus, J., Dahlman-Wright, K., Carlstedt-Duke, J., and Gustafsson, J.-Å. (1992) *J. Steroid Biochem. Mol. Biol. 42*, 131−139.
25. Izatt, R. M., and Christensen, J. J. (1976) in *CRC Handbook of Biochemistry and Molecular Biology: Physical and Chemical Data* (Fasman, G. D., Ed.) pp 151−269, CRC Press, Cleveland, OH.
26. Markley, J. (1975) *Acc. Chem. Res. 8*, 70−80.
27. Beres, L., and Sturtevant, J. M. (1971) *Biochemistry 10*, 2120−2126.
28. Murphy, K. P., Xie, D., Garcia, K. C., Amzel, L. M., and Freire, E. (1993) *Proteins 15*, 113−120.

BI000231I